for its hospitality and services provided during the final stages of this work. A predoctoral fellowship from the National Science Foundation, which I held throughout my graduate career, is gratefully acknowledged. This work has been directly supported by the National Science Foundation and the Office of Naval Research. In addition it has benefited from general support to the Material Sciences at the University of Chicago by the Advanced Research Projects Agency.

APPENDIX

Consider the equation

$$\langle e^{i\mathbf{k}\cdot\mathbf{y}_\nu}e^{i\mathbf{k}\cdot\mathbf{y}_\mu}\rangle_p=1+\langle\tfrac{1}{2}[(i\mathbf{k}\cdot\mathbf{y}_\nu)(i\mathbf{k}\cdot\mathbf{y}_\mu)]^2\rangle_p+\cdots. \quad \text{(A1)}$$

The terms with an odd number of factors of $\mathbf{y}$ go to zero because they contain products of an odd number of creation and/or destruction operators.

Since $\langle i\mathbf{k}\cdot\mathbf{y}_\nu\rangle_p$ is small compared to unity, (A1) can be written as

$$\langle e^{i\mathbf{k}\cdot\mathbf{y}_\nu}e^{i\mathbf{k}\cdot\mathbf{y}_\mu}\rangle_p=e^{-W}e^{-W'}e^{\frac{1}{2}(i\mathbf{k}\cdot\mathbf{y}_\mu i\mathbf{k}\cdot\mathbf{y}_\nu+i\mathbf{k}\cdot\mathbf{y}_\nu i\mathbf{k}\cdot\mathbf{y}_\mu)}$$
$$=e^{-W}e^{-W'}+e^{-W}e^{-W'}\times\tfrac{1}{2}\langle i\mathbf{k}\cdot\mathbf{y}_\mu i\mathbf{k}\cdot\mathbf{y}_\nu+i\mathbf{k}\cdot\mathbf{y}_\nu i\mathbf{k}\cdot\mathbf{y}_\mu\rangle_p,$$

where W refers to the νth atom and W' refers to the μth atom.

Equation (3.8) and the properties of creation and destruction operators give

$$\tfrac{1}{2}\langle i\mathbf{k}\cdot\mathbf{y}_\mu i\mathbf{k}\cdot\mathbf{y}_\nu+i\mathbf{k}\cdot\mathbf{y}_\nu i\mathbf{k}\cdot\mathbf{y}_\mu\rangle=\sum_{\mathbf{q}s}(\hbar/2MN\omega_{\mathbf{q}s})$$
$$\times\{[\mathbf{k}\cdot\mathbf{e}_{\mathbf{q}sb}][\mathbf{k}\cdot\mathbf{e}_{\mathbf{q}sb'}](\bar{n}_{\mathbf{q}s}+1)e^{i\mathbf{q}\cdot(\mathbf{R}_\nu{}^0-\mathbf{R}_\mu{}^0)}+\text{c.c.}\}. \quad \text{(A2)}$$

PHYSICAL REVIEW VOLUME 187, NUMBER 3 15 NOVEMBER 1969

Phase-Shift Analysis of the Fermi Surface of Copper

MARTIN J. G. LEE
The James Franck Institute and Department of Physics, The University of Chicago, Chicago, Illinois 60637

(Received 17 April 1969)

In an earlier paper a method was described whereby the partial-wave phase shifts that characterize the interaction between the conduction electrons and the lattice in a metal may be derived from experimental Fermi-surface data. In the present paper we apply the method of phase-shift analysis to study the shape of the Fermi surface of copper, which is known to be strongly perturbed by the *d*-like energy bands that lie almost 2 eV below the Fermi level. By adjusting the values of the *s*, *p*, *d*, and *f* phase shifts, and the Fermi-energy parameter, we construct a model Fermi surface on which the areas of the ⟨100⟩ belly and the ⟨111⟩ neck and belly orbits, the dog's bone, the four-cornered rosette, and the lemon orbit, are in good agreement with the results of precision measurements of the corresponding de Haas–van Alphen frequencies. The belly anisotropy of the model surface is also in good agreement with the experimental data, and the volume enclosed by the surface does not differ significantly from 1 electron/atom. The radii of the Fermi surface of copper in the (100) and (110) symmetry zones are determined to an accuracy of ±0.1%, and the results are in good agreement with the radii recently deduced by Halse by an independent technique. It is shown that the numerical values of the phase shifts are consistent with the position of copper in the Periodic Table. The local potential of Chodorow for Cu^+ produces phase shifts that are in substantial agreement with the results of the present work. A simple nonlocal correction to the Chodorow potential is proposed, such that the Fermi surface derived from the modified potential is entirely consistent with the experimental data. The energies associated with certain optical transitions in metallic copper are computed from the modified potential, and are found to agree with the results of recent piezo-optical experiments to better than 0.2 eV. It is concluded that the method of phase-shift analysis is capable of representing accurately the form of the *d*-like electronic energy bands in metals, and that the modified Chodorow potential may well prove to be the best starting point for a full calculation of the band structure of copper in the vicinity of the Fermi level.

I. INTRODUCTION

AS a result of several experimental investigations,[1–9] the geometry of the Fermi surface of copper is now known in substantial detail. Copper crystallizes in a fcc structure, and single crystals of copper may readily be grown with the high degree of chemical and structural perfection necessary for Fermi-surface studies by resonance techniques. According to the free-electron model, one would expect the Fermi surface of copper to be spherical and to lie entirely within the first Brillouin zone, which for the fcc Bravais lattice is a

[1] A. B. Pippard, Phil. Trans. Roy. Soc. (London) **A250**, 325 (1957).
[2] Yu. P. Gaĭdukov, Zh. Eksperim. i Teor. Fiz. **37**, 1281 (1959) [English transl.: Soviet Phys.—JETP **10**, 913 (1960)].
[3] D. Shoenberg, Phil. Trans. Roy. Soc. (London) **A255**, 85 (1962).
[4] H. V. Bohm and V. J. Easterling, Phys. Rev. **128**, 1021 (1962).
[5] A. S. Joseph, A. C. Thorsen, E. Gertner, and L. E. Valby, Phys. Rev. **148**, 569 (1966).
[6] I. M. Templeton, Proc. Roy. Soc. (London) **A292**, 413 (1966).
[7] J.-P. Jan and I. M. Templeton, Phys. Rev. **161**, 556 (1967).
[8] W. J. O'Sullivan and J. E. Schirber, Phys. Rev. **170**, 667 (1968); *ibid.*, Addendum (to be published).
[9] M. R. Halse, thesis, University of Cambridge, 1968 (unpublished); and Phil. Trans. Roy. Soc. (London) **A265**, 507 (1969).

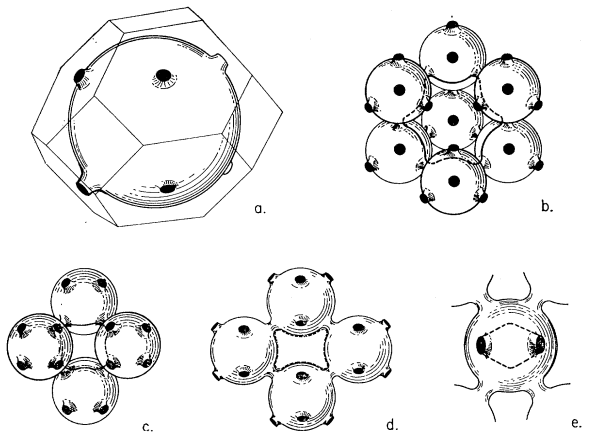

FIG. 1. Fermi surface of copper. (a) Schematic illustration of the Fermi surface of copper mapped in the reduced zone scheme. (b) Six-cornered rosette mapped in the extended zone scheme; broken lines indicate segments of the orbit that lie on the lower surfaces of the distorted spheres. (c) Four-cornered rosette in the extended zone scheme. (d) Dog's-bone orbit in the extended zone scheme. (e) Lemon orbit.

truncated octahedron. The anomalous skin effect studies of Pippard,[1] and the early de Haas–van Alphen effect studies of Shoenberg,[3] demonstrated that in fact the Fermi surface of copper is substantially distorted from the free-electron sphere. The surface bulges out along the ⟨111⟩ directions and contacts the Brillouin-zone boundary over a small region about the center of each hexagonal face, as is illustrated schematically in Fig. 1(a).

Of the experimental techniques of Fermiology, studies of the de Haas–van Alphen effect have contributed most to our present knowledge of the shape of the Fermi surface of copper. A de Haas–van Alphen frequency F may be defined by expressing the phase ϕ of the de Haas–van Alphen oscillations of magnetization in the form

$$\phi = 2\pi F/B,$$

where B is the magnetic flux density. Each experimentally observed frequency corresponds to an extremal orbit on the Fermi surface in a plane normal to the magnetic field, the frequency F being related to the area A of the orbit by the equation $F = (\hbar A/2\pi e)$. The Fermi surface of copper is multiply connected when mapped in the extended-zone scheme, and this results in several noncentral extremal orbits on the Fermi surface, each of which contributes to the de Haas–van Alphen effect. The geometries of some of these extremal orbits normal to symmetry directions are illustrated in Figs. 1(b)–1(e).

From the experimental de Haas–van Alphen data one can determine directly the extremal cross-sectional areas of the Fermi surface, but in order to calculate the radius vectors of the Fermi surface it is necessary to construct some model surface whose extremal cross-sectional areas can be fitted to the experimental data. Shoenberg's studies of the de Haas–van Alphen effect in copper led Roaf[10] to propose an analytic expression to represent the shape of the Fermi surface. He derived this expression by expanding the electronic energy in wave-vector space as a three-dimensional Fourier sum, the coefficients of which were adjusted to bring the cross-sectional areas of a surface of constant energy in wave-vector space into coincidence with the experimental Fermi-surface data. An alternative approach to the inversion of de Haas–van Alphen data has been discussed by Zornberg and Mueller,[11] who employed a model surface of which the cross-sectional areas were expanded as a sum of cubic harmonics with adjustable coefficients, and from which the radii could be deduced by a simple calculation.

In the course of recent studies of pressure effects on the Fermi surfaces of noble metals, Jan and Templeton[7] and O'Sullivan and Schirber[8] have made precision measurements of the absolute de Haas–van Alphen frequencies corresponding to several symmetry orbits on the Fermi surface of copper. Their results are set out in Table I. Detailed investigations of the anisotropies of the de Haas–van Alphen frequencies in copper have been carried out by Joseph, Thorsen, Gertner, and Valby,[5] and by Halse.[9] Halse interpreted the results of this work by recalculating the coefficients of Roaf's formula, and found it desirable to include a further term in the Fourier sum in order to obtain improved agreement with the experimental data. The estimated accuracy of the radii of the Fermi surface of copper deduced from Halse's final model surface is about $\pm 0.1\%$.

Theoretical studies of the electronic structure of copper have contributed greatly to the development of methods of band-structure calculation. The first-principles band-structure calculations of Segall[12] by the method of Korringa and Kohn and Rostocker[13] (KKR), and of Burdick,[14] by the augmented-plane-wave (APW) method of Slater,[15] predicted Fermi surfaces in satisfactory agreement with the experimental data then available, and incidentally demonstrated the equivalence of KKR and APW calculations based on the same potential. More recently, Snow and Waber[16] have carried out self-consistent energy-band calculations for copper, in an attempt to determine how best to represent the exchange potential that acts on the conduction electrons. Faulkner, Davis, and Joy[17] have computed

[10] D. J. Roaf, Phil. Trans. Roy. Soc. (London) **A255**, 135 (1962).
[11] E. I. Zornberg and F. M. Mueller, Phys. Rev. **151**, 557 (1966).
[12] B. Segall, Phys. Rev. **125**, 109 (1962).
[13] J. Korringa, Physica **13**, 392 (1947); W. Kohn and N. Rostoker, Phys. Rev. **94**, 1111 (1954); F. S. Ham and B. Segall, *ibid.* **124**, 1786 (1961).
[14] G. A. Burdick, Phys. Rev. **129**, 138 (1963).
[15] J. C. Slater, Phys. Rev. **51**, 846 (1937); **92**, 603 (1953).
[16] E. C. Snow and J. T. Waber, Phys. Rev. **157**, 570 (1967); E. C. Snow, *ibid.* **171**, 785 (1968).
[17] J. S. Faulkner, H. L. Davis, and H. W. Joy, Phys. Rev. **161**, 656 (1967); H. L. Davis, J. S. Faulkner, and H. W. Joy, *ibid.* **167**, 601 (1968).

constant-energy surfaces for copper, starting from various potentials, and have found results in good qualitative agreement with the experimental Fermi-surface data.

The distortions of the Fermi surfaces of real metals from a free-electron sphere are caused by an interaction between the conduction electrons and the lattice. Recently, attempts have been made to analyze the experimental Fermi-surface data in order to obtain information about the electron-ion interaction in metals. The pseudopotential method, in both its local[18] and its nonlocal[19] forms, has been applied to analyze the Fermi-surface distortions of several nearly-free-electron metals. However, these methods are inappropriate for a discussion of Fermi surfaces that involve or are strongly perturbed by d-like energy bands, since for d states the approximations of pseudopotential theory are known to fail.[20] In order to study the Fermi surfaces of metals of the d-transition series, including the noble metals, some alternative technique is required. Hodges, Ehrenreich, and Lang,[21] and Mueller,[22] have proposed interpolation schemes in which the conduction bands are treated in the nearly-free-electron approximation, while the d states are represented by tight-binding functions. The hybridization integrals and overlap integrals are treated as adjustable parameters, and are determined by fitting the model Hamiltonian to the results of first-principles band-structure calculations. The interpolation schemes are economical in computer time and are capable of giving an excellent over-all fit to the results of energy-band calculations. However, since they involve a large number of adjustable parameters, they are not easily applied to the interpretation of experimental Fermi-surface data. The interpolation schemes have been discussed in detail by Heine[23] and by Phillips.[24]

A method has recently been described whereby the partial-wave phase shifts that characterize the interaction between the conduction electrons and the ionic cores in a metallic lattice may be derived from experimental Fermi-surface data. In an earlier paper[25] the method of phase-shift analysis was described and was applied to a discussion of the shapes of the Fermi surfaces of metals of the alkali series. The alkali metals have nearly-free-electron energy bands and nearly spherical Fermi surfaces. For these metals, phase-shift analysis is an alternative to pseudopotential analysis, with the advantage of rapid convergence of the fitting procedure and direct physical interpretation of the parameters, but with the disadvantage of requiring more elaborate programming and more costly computing.

TABLE I. Precision experimental measurements of the de Haas-van Alphen frequencies of some symmetry orbits in copper.

Orbit	Notation	Experimental frequency (10^8 G)
Belly	B_{100}	(5.998±0.006)[a]
Belly	B_{111}	(5.814±0.006)[a]
		(5.809±0.006)[b]
Neck	N_{111}	(0.2177±0.0002)[a]
		(0.2174±0.0002)[b]
Dog's bone	D_{110}	(2.514±0.003)[a]
4-rosette	R_{100}	(2.462±0.003)[a]
6-rosette	R_{111}	
Lemon	L_{110}	(2.194±0.006)[c]

[a] Reference 8.
[b] Reference 7.
[c] K. A. McEwen and J. Vanderkooy (private communication).

In the present paper we explore further the validity of the method of phase-shift analysis by applying it to experimental data relating to the Fermi surface of copper. The shape of the Fermi surface of copper is known to be strongly perturbed by the d bands that lie about 2 eV below the Fermi level and hybridize with the conduction band. By a detailed study of the extent to which the experimental Fermi surface of copper may be described by phase-shift analysis, we hope to determine whether the method is capable of representing accurately the form of d-like energy bands in solids, and hence to judge whether the method might reasonably be applied to an analysis of the Fermi surfaces of metals of the d-transition series.

The paper is divided into five sections. In Sec. II, the method of calculation is outlined; in Sec. III, the results of the calculation are presented, and finally in Secs. IV and V the results and conclusions of the present work are discussed.

II. METHOD OF CALCULATION

The present analysis of the experimentally observed distortions of the Fermi surface of copper follows closely the technique previously described.[25] For this reason we describe only in outline the method of calculation; for a more detailed discussion the reader is referred to the earlier paper.

Under certain approximations the Dyson equation, whose solutions represent the quasiparticle excitations of a system of nonrelativistic interacting electrons in thermal equilibrium with an ionic lattice, reduces to a single-particle-like Schrödinger equation in which exchange and correlation effects are folded into a nonlocal (energy and angular-momentum dependent) effective potential. This equation is of the form

$$[-(\hbar^2/2m)\nabla^2+V_{\rm eff}(\mathbf{r},l,E)]\phi_{n,\mathbf{k}}(\mathbf{r})=E_n(\mathbf{k})\phi_{n,\mathbf{k}}(\mathbf{r}), \quad (1)$$

[18] N. W. Ashcroft, Phil. Mag. **8**, 2055 (1963); M. J. G. Lee, Proc. Roy. Soc. (London) **A295**, 440 (1966).
[19] J. C. Kimball, R. W. Stark, and F. M. Mueller, Phys. Rev. **162**, 600 (1967); M. J. G. Lee and L. M. Falicov, Proc. Roy. Soc. (London) **A304**, 319 (1968).
[20] W. A. Harrison, *Pseudopotentials in the Theory of Metals* (W. A. Benjamin, Inc., New York, 1966), p. 7.
[21] L. Hodges, H. Ehrenreich, and N. D. Lang, Phys. Rev. **152**, 505 (1966).
[22] F. M. Mueller, Phys. Rev. **148**, 636 (1966).
[23] V. Heine, Phys. Rev. **153**, 673 (1967).
[24] J. C. Phillips, Advan. Phys. **17**, 79 (1968).
[25] M. J. G. Lee, Phys. Rev. **178**, 953 (1969).

TABLE II. (a) Phase shifts for copper from experimental data, setting f and higher phase shifts equal to zero. (b) Illustrating the effect on the best values of the s, p and d phase shifts of assuming a small positive f phase shift. Energies are expressed in Ry, and phase shifts in rad.

E_F	η_0	η_1	η_2	η_3	η_4
		(a)			
0.52	0.1343	0.1514	−0.1051	0	
0.54	0.0961	0.1372	−0.1136	0	
0.56	0.0588	0.1224	−0.1224	0	
0.58	0.0224	0.1071	−0.1314	0	
0.60	−0.0131	0.0912	−0.1407	0	
		(b)			
0.56	0.0588	0.1224	−0.1224	0	0
0.56	0.0451	0.1180	−0.1202	0.0010	0

and the approximations involved in its derivation are such that one would expect it to describe accurately the shape of the Fermi surface of a metal, and the form of the energy bands close to the Fermi energy.

The one-particle-like Schrödinger equation (1) is solved for the shapes of surfaces of constant energy in wave-vector space, and the scattering phase shifts associated with the effective potential are adjusted to bring appropriate features of the computed Fermi surface into agreement with the experimental data. The effective one-electron potential is assumed to be of muffin-tin form; that is, radially symmetric within nonintersecting spheres centered on each lattice site, and constant elsewhere.

The inclusion of relativistic effects would introduce three new terms into the nonrelativistic Schrödinger equation.[26] Of these, the relativistic mass-velocity correction and the Darwin term may be folded into a nonlocal effective potential, but the spin-orbit interaction cannot be treated in this way. While it is not difficult to include spin-orbit effects in a phase-shift analysis of experimental Fermi-surface data, their influence on the shape of the Fermi surface of copper is believed to be negligible. Our reasons for neglecting the spin-orbit interaction in the present work are discussed in more detail below.

Either the KKR method or the APW method might be applied to solve the nonrelativistic Schrödinger equation (1) for a potential of muffin-tin form; in the present calculations the APW method was employed. It is convenient to set the constant potential between the muffin-tin spheres equal to zero, so defining the APW scale of energy. A standard variational calculation for a muffin-tin potential[27] leads to the following dispersion relation for conduction electrons in a crystalline lattice. The electronic energy bands $E_n(\mathbf{k})$ are solutions of the secular equation

$$\det[((\mathbf{k}+\mathbf{g})^2-E)\delta_{\mathbf{g}\mathbf{g}'}+\Gamma_{\mathbf{g}\mathbf{g}'}(\mathbf{k},E)]=0, \quad (2)$$

where for a primitive crystal lattice

$$\begin{aligned}\Gamma_{\mathbf{g}\mathbf{g}'}(\mathbf{k},E)&=(4\pi R_s^2/\Omega)\{-[(\mathbf{k}+\mathbf{g}')\cdot(\mathbf{k}+\mathbf{g})-E]\\&\times j_1(|\mathbf{g}-\mathbf{g}'|R_s)/|\mathbf{g}-\mathbf{g}'|\\&+\sum_{l=0}^{\infty}(2l+1)P_l(\cos\theta_{\mathbf{g}\mathbf{g}'})j_l(|\mathbf{k}+\mathbf{g}|R_s)\\&\times j_l(|\mathbf{k}+\mathbf{g}'|R_s)[\mathfrak{R}_l'(R_s,E)/\mathfrak{R}_l(R_s,E)]\}. \quad (3)\end{aligned}$$

In this equation, $\mathbf{g}$ and $\mathbf{g}'$ are reciprocal-lattice vectors of the Bravais lattice, R_s is the radius of the spherical component of the muffin-tin potential, Ω is the atomic volume, $\theta_{\mathbf{g}\mathbf{g}'}$ is the angle between the vectors $(\mathbf{k}+\mathbf{g})$ and $(\mathbf{k}+\mathbf{g}')$,[28] and $[\mathfrak{R}_l'(R_s,E)/\mathfrak{R}_l(R_s,E)]$ is the logarithmic derivative of the solution of the radial Schrödinger equation for angular momentum l, such that

$$-\frac{1}{r^2}\frac{\partial}{\partial r}\left(\frac{r^2\partial\mathfrak{R}_l(r,E)}{\partial r}\right)+\left[\frac{l(l+1)}{r^2}+V_{\text{eff}}(r,l,E)\right]\mathfrak{R}_l(r,E)=E\mathfrak{R}_l(r,E), \quad (4)$$

evaluated at the muffin-tin radius. The effective potential $V_{\text{eff}}(r,l,E)$ enters into the secular determinant (2) only to the extent that it determines the logarithmic derivatives of the radial wave functions.

In a first-principles APW band-structure calculation, the logarithmic derivatives of the radial wave functions that correspond to some assumed effective potential are first computed by numerical integration of the radial Schrödinger equation (4). The logarithmic derivatives are then substituted into (3) and the energy

TABLE III. Extremal cross-sectional areas (in free-electron units) of the Fermi surface of copper. Comparison of areas of extremal orbits in symmetry directions computed from the phase-shift model with the areas derived from experimental measurements of absolute de Haas–van Alphen frequencies.

		Computed	Experimental
Belly	B_{100}[a]	0.9807 ±0.0002	0.9810 ±0.0010[b]
Belly	B_{111}[a]	0.9503 ±0.0001	0.9510 ±0.0010[b]
			0.9498 ±0.0010[c]
Neck	N_{111}[a]	0.03557±0.00001	0.03561±0.00004[b]
			0.03556±0.00004[c]
Dog's bone	D_{110}	0.4106 ±0.0003	0.4112 ±0.0004[b]
4-rosette	R_{100}	0.4021 ±0.0001	0.4027 ±0.0005[b]
6-rosette	R_{111}	1.7997 ±0.0003	
Lemon	L_{110}	0.3590 ±0.0004	0.359 ±0.001[d]

[a] Fitting parameters.
[b] Reference 8.
[c] Reference 7.
[d] K. A. McEwen and J. Vanderkooy (private communication).

[26] T. L. Loucks, Phys. Rev. **139**, 231 (1965); D. Koelling, Quarterly Progress Report No. 68, Solid State and Molecular Theory Group, Massachusetts Institute of Technology, 1968 (unpublished).

[27] For an introduction to many of the practical aspects of the APW method, and for a guide to the literature, see T. Loucks, *The Augmented Plane Wave Method* (W. A. Benjamin, Inc., New York, 1967).

[28] Note that in Ref. 25, $\theta_{\mathbf{g}\mathbf{g}'}$ was erroneously stated to be the angle between the reciprocal-lattice vectors $\mathbf{g}$ and $\mathbf{g}'$.

TABLE IV. (a) Illustrating the sensitivity of the computed central-belly anisotropy parameters D_1, D_2, and D_3 to the values of η_3 and E_F. The anisotropy parameters are defined in the text. (b) The closest agreement with the experimental data was obtained with the set of phase shifts (4) of (a). The corresponding anisotropy parameters are shown.

	E_F(Ry)	η_0	η_1	η_2	η_3	D_1	D_2	D_3
				(a)				
(1)	0.56	0.0588	0.1224	−0.1224	0	−0.00606	−0.00319	+0.0208
(2)	0.56	0.0451	0.1180	−0.1202	0.0010	−0.00633	−0.00341	+0.0205
(3)	0.60	−0.0131	0.0912	−0.1407	0	−0.00622	−0.00335	+0.0203
(4)	0.55	0.0581	0.1235	−0.1150	0.0014	−0.00647	−0.00349	+0.0203

(b)

	Computed	Experimental
D_1	(−0.00647±0.00010)	(−0.00669)[a]
		(−0.00645±0.00010)[b]
D_2	(−0.00349±0.00006)	(−0.00332)[a]
		(−0.00342±0.00010)[b]
D_3	(+0.0203 ±0.0005)	(−0.0212)[a]
		(−0.0196 ±0.0006)[b]

[a] Reference 5. [b] Reference 9.

bands are computed from the roots of the secular determinant (2). The method of phase-shift analysis is closely related to such a calculation. Here the logarithmic derivatives are regarded as adjustable parameters in terms of which the shapes of surfaces of constant energy in wave-vector space may be computed. The values of the logarithmic derivatives are determined by bringing the constant energy surface computed from Eqs. (2), (3), and (4) into coincidence with the experimentally observed Fermi surface.

Since the muffin-tin potential is of finite range, the logarithmic derivatives of the radial wave function may be related to the partial-wave scattering phase shifts $\eta_l(E)$ of the effective potential, by the equation

$$\frac{\mathfrak{R}_l'(R_s,E)}{\mathfrak{R}_l(R_s,E)}=\left[\frac{j_l'(kr)-\tan\eta_l(E)y_l'(kr)}{j_l(kr)-\tan\eta_l(E)y_l(kr)}\right]_{r=R_s}, \quad (5)$$

where $k^2=E$. Since only the tangents of the phase shifts enter into (5), the shape of the surface of constant energy E in wave-vector space is fully determined by the corresponding set of "reduced" phase shifts $\eta_l(E)$ from which all integer multiples of π have been subtracted. In practice, it is convenient to consider the phase shifts, rather than the logarithmic derivatives, as the adjustable parameters. In what follows we shall often refer to the phase shifts for $l=0$, 1, 2, 3, as the s, p, d, and f phase shifts, respectively.

Digital computer programs have been developed to calculate the radii and the cross-sectional areas of surfaces of constant energy in wave-vector space, for a given energy E and a given set of reduced phase shifts $\eta_l(E)$. The numerical techniques employed in these calculations have been described elsewhere.[25] In the present calculations the phase shifts $\eta_l(E)$ for $l=0$, 1, 2, and 3 were treated as adjustable parameters, the phase shifts for $l=4$–8 were set equal to zero, and the summation over l in Eq. (3) was truncated beyond $l=8$. The calculations were carried out with a 30×30 secular determinant, since this was found to give satisfactory convergence. The approximations and convergence of the present calculations are discussed in more detail below.

III. RESULTS

In order to compute the shape of the Fermi surface from Eqs. (2)–(4), we must set the energy parameter E in the secular determinant (2) equal to the Fermi energy on the APW scale (E_F). But initially we have no knowledge of the correct value of E_F, and for this reason the phase-shift calculations were carried out for a series of values of E_F, the range of energies being guided by the results of first-principles APW calculations. At each energy the s, p, and d phase shifts were adjusted to bring the computed cross-sectional areas of the ⟨100⟩ central-belly orbit, and the ⟨111⟩ central-belly and neck orbits, into agreement with the experimental data (Table I). For a given value of the Fermi-energy parameter, the phase shifts are determined uniquely by this procedure. The sets of phase shifts deduced in this way are presented in Table II. It will be seen that the computed phase shifts depend sensitively on the assumed value of E_F.

The areas of the dog's bone, four-cornered rosette, six-cornered rosette, and lemon orbits were computed for each set of phase shifts. We found that, on the scale of the experimental accuracy, the absolute areas of these orbits do not depend significantly on the assumed value of E_F. In Table III, the computed areas are compared with the areas derived from precision measurements of the de Haas–van Alphen frequencies associated with the various symmetry orbits.[29] Wherever comparison with experimental data is possible, the agreement is satisfactory.

[29] The lattice constant assumed in reducing the data to free electron units was that quoted by Halse (Ref. 9), namely, $a_0=(3.6030\pm0.0003)$ Å at 1°K. The corresponding value of the extremal cross-sectional area of the free-electron sphere is $A_0=5.8363$ Å^{-2}.

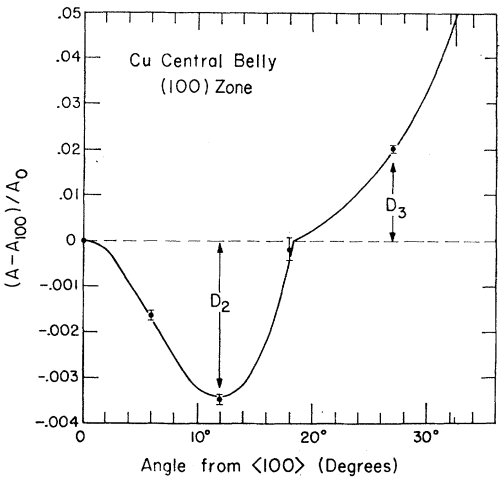

FIG. 2. Anisotropy of the central extremal cross-sectional area of the Fermi surface of copper normal to directions in the (100) zone. The continuous curve represents the experimental data of Halse (Ref. 9). The points represent the area distortions computed as described in the text. Error bars associated with the points represent the combined error of experiment and computation. Note the change of the vertical scale above and below the horizontal axis. A_0 is the extremal cross-sectional area of the free-electron sphere (Ref. 29).

In a further calculation, also presented in Table II, the f phase shift was assigned a small positive value.[30] It was found that the magnitudes of the s, p, and d phase shifts depend sensitively on the value assigned to η_3; however, the computed areas of the symmetry orbits are not sufficiently sensitive to the magnitude of η_3 to allow one to determine the best value of this parameter.

Thus current experimental measurements of the absolute de Haas–van Alphen frequencies associated with the symmetry orbits in copper are not sufficiently accurate to allow one to determine with any precision the best values of the Fermi energy parameter and the f phase shift. However, the computed values of the belly-anisotropy parameters D_1, D_2, and D_3, which are defined by

$$D_1 = \text{area } (16° \text{ from } \langle 100\rangle \text{ in } (110) \text{ zone} - B_{100}),$$
$$D_2 = \text{area } (12° \text{ from } \langle 100\rangle \text{ in } (100) \text{ zone} - B_{100}),$$
$$D_3 = \text{area } (27° \text{ from } \langle 100\rangle \text{ in } (100) \text{ zone} - B_{100}),$$

turn out to be significantly sensitive to the values of E_F and η_3. This is illustrated by the results set out in Table IV. By adjusting E_F and η_3 to bring the computed values of D_1, D_2, and D_3 into closest agreement (in a least-squares sense) with the experimental data, one might deduce the best set of phase shifts, and also the best value of E_F.

[30] The value of the f phase shift assumed in this calculation ($\eta_3 = 0.0010$ rad) is close to that obtained by numerical integration of the radial Schrödinger equation with the Chodorow potential (Ref. 32).

TABLE V. Radii (in free-electron units) of the Fermi surface of copper in symmetry zones.

Angle from ⟨100⟩	Present work	Cu 7[a]
	(100) zone	
0°	1.0586	1.059
5°	1.0490	1.049
10°	1.0273	1.027
15°	1.0042	1.004
20°	0.9848	0.985
25°	0.9704	0.970
30°	0.9607	0.960
35°	0.9549	0.954
40°	0.9520	0.952
45°	0.9511	0.951
	(110 zone)	
0°	1.0586	1.059
5°	1.0490	1.049
10°	1.0276	1.027
15°	1.0058	1.006
20°	0.9900	0.990
25°	0.9827	0.983
30°	0.9854	0.986
35°	1.0000	1.000
40°	1.0311	1.031
45°	1.1175	1.117
50°	neck	neck
55°	neck	neck
60°	neck	neck
65°	1.0935	1.094
70°	1.0214	1.022
75°	0.9872	0.987
80°	0.9664	0.966
85°	0.9549	0.955
90°	0.9511	0.951

[a] Reference 9.

Our final set of phase shifts is set out in Table IV. This set of phase shifts leads to values of the belly-anisotropy parameters that are in satisfactory agreement with the experimental data, but no attempt was made to refine the phase shifts by a least-squares

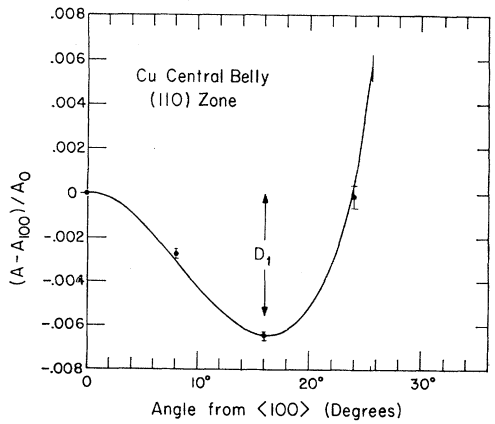

FIG. 3. Anisotropy of the central extremal cross-sectional area of the Fermi surface of copper normal to directions in the (110) zone. The continuous curve represents the experimental data of Halse (Ref. 9). The points represent the area distortions computed as described in the text. Error bars associated with the points represent the combined error of experiment and computation.

TABLE VI. (a) Convergence of the phase shifts as the size of the secular determinant is increased. The size of the determinant is $n\times n$. (b) Convergence of the phase shifts for increasing values of the parameter l_{max}. (c) Sensitivity of the computed phase shifts to variations in the assumed radius R_s of the muffin-tin sphere. The phase shifts are expressed in rad. R_I is the inscribed sphere radius ($R_I=2.4072$ a.u.). R_{ws} is the Wigner-Seitz radius ($R_{ws}=2.6602$ a.u.).

n	η_0	η_1	η_2	η_3
		(a)		
20	0.0589	0.1233	−0.1126	0.0014
30[a]	0.0581	0.1235	−0.1150	0.0014
40	0.0575	0.1234	−0.1154	0.0014
50	0.0573	0.1234	−0.1156	0.0014
60	0.0574	0.1234	−0.1157	0.0014
		(b)		
l_{max}	η_0	η_1	η_2	η_3
6	0.0581	0.1238	−0.1159	0.0014
8[a]	0.0581	0.1235	−0.1150	0.0014
10	0.0581	0.1235	−0.1150	0.0014
12	0.0581	0.1235	−0.1150	0.0014
		(c)		
R_s(a.u.)	η_0	η_1	η_2	η_3
2.18	0.0632	0.1239	−0.1134	0.0014
2.29	0.0598	0.1236	−0.1144	0.0014
2.41(R_I)[a]	0.0581	0.1235	−0.1150	0.0014
2.53	0.0581	0.1235	−0.1158	0.0014
2.66(R_{ws})	0.0577	0.1237	−0.1156	0.0014

[a] Denotes the parameters adopted for the calculations set out in previous tables.

calculation. A more elaborate calculation might reduce somewhat the error associated with η_3 and E_F, but such a calculation is probably not worthwhile in view of the relatively large discrepancies between the experimental belly-anisotropy parameters given by Joseph, Thorsen, Gertner and Valby,[5] and those given by Halse.[9] In Figs. 2–4 the angular variations of the central-belly frequency in the (100) and (110) symmetry zones, and of the neck frequency in the (110) zone, are compared with the experimental results of Halse. The agreement here is satisfactory. The volume enclosed by the computed Fermi surface was determined by graphical integration, and was found to be (1.000±0.003) electrons/atom.

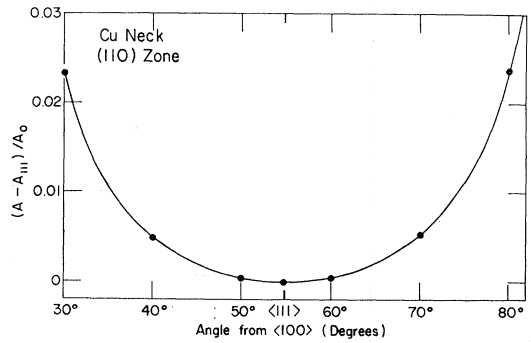

FIG. 4. Anisotropy of the extremal cross-sectional area of the neck of the Fermi surface of copper normal to directions in the (110) zone. The continuous curve represents the experimental data of Halse (Ref. 9). The points represent the areas of the computed surface. Although no explicit estimate of the experimental accuracy is available, there appears to be no significant discrepancy between the computed surface and the experimental data.

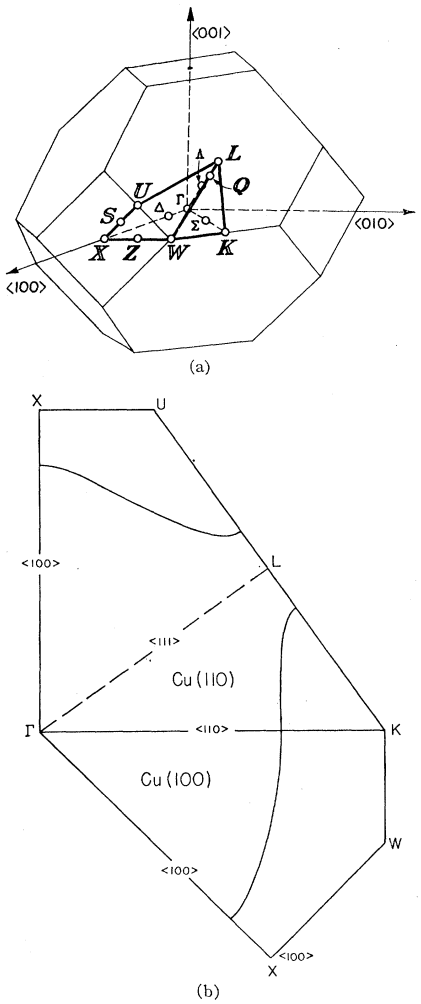

FIG. 5. (a) The standard notation for symmetry lines and symmetry points in the first Brillouin zone of the fcc Bravais lattice. (b) The extremal cross sections of the Fermi surface of copper normal to the ⟨100⟩ and ⟨110⟩ symmetry directions, as computed in the course of the present work.

The good agreement between the cross-sectional areas of the computed surface, and the experimental data, suggests that the computed surface may well represent a satisfactory model from which the radii of the Fermi surface of copper might be calculated. In Fig. 5(a), the conventional notation for symmetry points in the first Brillouin zone of copper is indicated. In Fig. 5(b), the central cross sections of the model surface in the (100) and (110) symmetry zones are presented, and in Table V the radii in these two zones are compared with the radii computed by Halse using the inversion scheme of Roaf.[10] The agreement between the results of the two calculations encourages some confidence in the final radii, since the two methods of

TABLE VII. Comparison of published estimates of the radii of the Fermi surface of copper ($Å^{-1}$).

	B_{100}	B_{110}	N
First-principles calculations			
Segall[a]	1.43	1.29	0.20
Segall[b]	1.39	1.26	0.28
Snow and Waber[c]	1.36	1.28	0.22
Snow and Waber[d]	1.44	1.14	0.38
Faulkner *et al.*[e]	1.427	1.298	0.242
Faulkner *et al.*[f]	1.431	1.297	0.246
Faulkner *et al.*[g]	1.448	1.281	0.292
Snow[h]	1.36	1.30	none
Snow[i]	1.39	1.29	0.31
Interpretations of experimental data			
Roaf[j]	1.45	1.28	0.27
Roaf[k]	1.46	1.28	0.27
Bohm and Easterling[l]	1.41	1.30	0.265
Zornberg and Mueller[m]	1.43	1.33	0.26
Halse[n]	1.439	1.292	0.2562
Present work	1.438	1.292	0.2562[o]

[a] Chodorow potential (Ref. 12).
[b] l-dependent potential (Ref. 12).
[c] Self-consistent APW calculation including the exchange potential in Slater's free-electron approximation. Relativistic core wave functions (Ref. 16).
[d] Self-consistent APW calculation after reducing the exchange potential to $\frac{2}{3}$ of the Slater potential. Relativistic core wave functions (Ref. 16).
[e] KKR calculation based on the Chodorow potential and with $l_{max}=2$ (Ref. 17).
[f] KKR calculation based on the Chodorow potential and with $l_{max}=4$ (Ref. 17).
[g] KKR calculation based on a potential derived from atomic Hartree-Fock wave functions for copper as computed by Watson (Ref. 17).
[h] Self-consistent APW calculation including the exchange potential in Slater's free-electron approximation. Nonrelativistic core wave functions (Ref. 16).
[i] Self-consistent APW calculation after reducing the exchange potential to $\frac{2}{3}$ of the Slater potential. Nonrelativistic core wave functions (Ref. 16).
[j] Radii derived from Roaf's Cu IV fit to the experimental data of Shoenberg (Ref. 10).
[k] Radii derived from Roaf's Cu VI fit to the experimental data of Shoenberg (Ref. 10).
[l] Reference 4.
[m] Reference 11.
[n] Radii derived from Halse's Cu 7 surface (Ref. 9).
[o] Mean neck radius: the extreme radial anisotropy of the neck of the computed surface is close to 1 part in 10^4, the radius along LW being greater than along LK and LU.

calculation are entirely different, and the two sets of fitting parameters are partially independent. Of these two methods, Roaf's inversion scheme is simpler to program and more economical in computer time. Phase-shift analysis involves fewer adjustable parameters, however, and the adjustable parameters (the phase shifts) have a more direct physical significance.

Accuracy of the Calculations

Several approximations are involved in our calculation of the scattering phase shifts from the experimental Fermi-surface data. The mesh associated with the interpolation procedure by which the Fermi radius in a given direction is determined, and that associated with the technique of numerical integration by which the cross-sectional areas of the computed surfaces are calculated, were adjusted so that errors in the computed areas are substantially smaller than errors in the experimental data. Nevertheless, errors associated with numerical integration limit the accuracy of the computed areas presented in Table III and in Table IV.

For the majority of calculations a 30×30 secular determinant was employed, all APW's being included in the basis set for which $|\mathbf{k}+\mathbf{g}|<6.0(\pi/a)$, where $\mathbf{k}$ is a wave vector on the free-electron Fermi sphere at the center of the (1/48)th sector of the Brillouin zone within which the calculations were carried out. The influence of the size of the secular determinant on the computed phase shifts is indicated in Table VI(a). Since the computed phase shifts are not significantly altered by doubling the size of the secular determinant, it was concluded that a 30×30 determinant is sufficiently large to ensure satisfactory convergence of the calculations. The sum over l in (3) was truncated beyond $l=8$. The results set out in Table VI(b) show that the final phase shifts are not significantly influenced by increasing the number of terms included in this summation.

The most critical approximation of the present calculations, in the sense that it is the most difficult to test and to improve upon, is the assumption that the experimental Fermi surface may be derived from a potential of muffin-tin form. In an attempt to estimate the errors involved in truncating the potential at the inscribed-sphere radius, we have computed the best set of phase shifts for a series of muffin-tin radii. From the results of these calculations as set out in Table VI(c) it will be seen that, over the range of radii we have investigated, the computed phase shifts are largely independent of the radius of the muffin-tin sphere. Any substantial dependence of the computed phase shifts on the muffin-tin radius would suggest that the experimental Fermi surface cannot be derived from a potential of muffin-tin form. Thus the muffin-tin approximation appears to be satisfactory for a phase-shift analysis of the Fermi surface of copper. The present results also confirm our earlier observation[25] that increasing the muffin-tin radius beyond the radius of the inscribed sphere does not introduce discontinuous changes in the computed phase shifts.

The errors associated with the computed phase shifts that describe the conduction electron-ion interaction in copper are dominated by experimental error in the fitting parameters, namely the ⟨100⟩ belly area, the ⟨111⟩ neck and belly areas, and the belly-anisotropy parameters D_1, D_2, and D_3. The errors in the phase shifts, as set out in (6) below, were computed under the assumption that the Fermi energy parameter is given by $E_F=0.550$ Ry. In fact, there is some uncertainty in our estimate of the best value of this parameter, and the computed phase shifts are rather sensitive to the value of E_F. If the phase shifts $\eta_l(E_F)$ and the Fermi energy parameter E_F are regarded as independently adjustable parameters, then this uncertainty in the value of E_F leads to a further large contribution to the estimated error in the phase shifts. However, independent adjustment of the $\eta_l(E_F)$ and E_F is not permissible, since there exists a unique relationship between the Friedel sum of the phase shifts,

which is defined by

$$\mathfrak{F}(E_F)=(2/\pi)\sum_{l=0}^{\infty}(2l+1)\eta_l(E_F)$$

and the value of the Fermi-energy parameter.[25] For this reason we prefer to express the present results as a relationship between the phase shifts and the assumed value of the Fermi energy parameter, and to regard as an independent result of the calculations our best estimate of the Fermi energy parameter:

$$E_F=(0.550\pm0.005)\text{ Ry}.$$

Setting $E_F=0.550$ Ry we find, after approximate correction for incomplete convergence of the secular determinant, the following estimates of the reduced phase shifts:

$$\begin{aligned}\eta_0&=(+0.0574\pm0.0042)\text{ rad},\\ \eta_1&=(+0.1234\pm0.0014)\text{ rad},\\ \eta_2&=(-0.1157\pm0.0009)\text{ rad},\\ \eta_3&=(+0.0014\pm0.0003)\text{ rad}.\end{aligned}\qquad(6)$$

If the energy dependence of the f phase shift is neglected, the best set of phase shifts corresponding to any other value of E_F may be estimated from the dependence of the phase shifts on the assumed value of the Fermi energy parameter, as given in Table II.

So far in our analysis of the shape of the Fermi surface of copper, we have omitted any discussion of the effects of spin-orbit interaction. The spin-orbit interaction mixes spinor components and introduces into the secular determinant (2) a further term that cannot be expressed analytically as a correction to the phase shifts. In general, the effect of spin-orbit interaction is to split any accidental degeneracies and orbital degeneracies that may be present in the nonrelativistic band structure. But there are no accidental degeneracies near the Fermi level in the band structure of copper, and the only orbital degeneracies that are likely to influence the Fermi surface are those associated with the L_3 and X_5 states in the d-band complex that lies about 0.15 Ry below the Fermi level.[12,14]

If we may take the spin-orbit splitting of the $3d$ states in the free copper atom (0.005 Ry)[31] as an order of magnitude estimate of the spin-orbit splitting of orbitally degenerate states in the metal, then a simple perturbation calculation shows that spin-orbit splitting is unlikely to shift the energy bands at the Fermi level by more than 2×10^{-4} Ry. The corresponding change in the Fermi wave vector is about an order of magnitude smaller than the error implied by experimental error in the de Haas–van Alphen frequency measurements. For this reason we believe that neglecting spin-orbit interaction is a valid approximation in the present work.

[31] C. E. Moore, *Atomic Energy Levels* (U. S. Government Printing Office, National Bureau of Standards, Washington, D. C. 1949).

TABLE VIII. Comparison of various estimates of the Fermi energy of copper measured on the APW scale.

Potential	E_F(Ry)
Chodorow[a,b]	0.555
l-dependent Segall[a]	0.717
Snow and Waber[c]	0.556
Snow[d,e]	0.503
Snow[e,f]	0.548
Present work	(0.550±0.005)

[a] Reference 12.
[b] Reference 14.
[c] Full Slater exchange; core charge-density derived from self-consistent relativistic Dirac-Slater wave functions (Ref. 16).
[d] Full Slater exchange; core charge density derived from nonrelativistic Hartree-Fock-Slater wave functions.
[e] E. C. Snow (private communication).
[f] Exchange potential reduced to $\frac{2}{3}$ of Slater's potential; core charge density derived from nonrelativistic Hartree-Fock-Slater wave functions.

IV. DISCUSSION

The final set of phase shifts (6) leads to a computed Fermi surface having the following characteristics. The areas of the ⟨100⟩ belly, the ⟨111⟩ neck and belly orbits, the dog's bone, the four-cornered rosette, and the lemon orbit, are in good agreement with the results of current precision measurements (Table III). The central-belly and neck anisotropies are in good agreement with the experimental results of Halse (Figs. 2–4). The radii of the model surface in the (100) and (110) symmetry zones are in excellent agreement with the radii computed by Halse, using the inversion technique of Roaf (Table V), and the volume enclosed by the surface does not differ significantly from the expected volume of 1 electron/atom.

In Table VII we summarize the results of recent calculations of the radii of the Fermi surface of copper along symmetry directions, some of which are based on first-principles calculations and others on the interpretation of experimental data. Of the first-principles calculations, the KKR calculation by Faulkner, Davis, and Joy,[17] in which the Chodorow potential[32] was assumed, leads to a Fermi surface whose radii are in the closest agreement with the present results. The various interpretations of the experimental data lead to results for the principal radii of the Fermi surface of copper that are consistent with one another within the accuracy of the various determinations. The close agreement between the radii deduced by Halse and the radii found in the course of the present work encourages some confidence in the results of the phase-shift analysis.

In a first-principles band-structure calculation by the APW method, the Fermi energy parameter E_F is determined by integrating the computed density of states to find that energy below which the total number of electronic states is equal to the number of conduction electrons in the metal. We compare in Table VIII our best estimate of the Fermi energy parameter with

[32] M. I. Chodorow, Ph.D. thesis, M. I. T., 1939 (unpublished); the potential used in the present work was obtained by interpolating the data quoted by Burdick (Ref. 14).

TABLE IX. (a) Comparison of reduced phase shifts at energy $E=0.550$ Ry. The phase shifts are expressed in radians. (b) Angular-momentum-dependent correction to the Chodorow potential required to bring the phase shifts at energy $E_F=0.550$ Ry into agreement with the phase shifts computed from the experimental Fermi-surface data. The correction is a constant δV within the muffin-tin sphere, and zero elsewhere. (c) Comparison between theory and experiment for the energies of certain optical transitions in copper. Energies are expressed in eV.

	Chodorow[a]	Snow and Waber[b]	Present work
		(a)	
0	+0.0404	−0.1758	(+0.0574±0.0042)
1	+0.1011	+0.0276	(+0.1234±0.0014)
2	−0.1202	−0.1112	(−0.1157±0.0009)
3	+0.0009	+0.0005	(+0.0014±0.0003)

(b)

l	$\delta V(l)$ Ry
0	(−0.0120±0.0030)
1	(−0.0353±0.0024)
2	(−0.0102±0.0029)
3	(−0.1560±0.0940)
⩾4	0

(c)

Source	$(E_F-L_3^{\text{upper}})$	$(X_4'-X_5)$	$(L_1^{\text{upper}}-E_F)$
Experiment[c]	(2.1±0.1)	(4.0±0.1)	(4.15±0.10)
Chodorow[d]	2.10	3.95	3.96
l-dependent[e]	2.3	4.7	5.15
Watson[f]	1.6	3.1	3.9
Snow and Waber[b]	3.2	5.5	...
Modified Chodorow (present work)	2.11	3.77	3.99

[a] Reference 31.
[b] Reference 16.
[c] Reference 33.
[d] Reference 12, 14.
[e] Reference 12.
[f] Reference 17.

estimates derived from first-principles calculations. The numerical value of E_F found in first-principles calculations appears to depend sensitively on the approximations that are involved in setting up the one-electron potential in the metal. In particular, the value of E_F derived from the self-consisted band-structure calculations of Snow[16] depends on the coefficient that is associated with the Slater exchange potential. Comparison between the values of E_F obtained in calculations by Snow, and Snow and Waber,[16] in each of which the full Slater exchange potential was assumed, shows that the computed value of E_F is sensitive also to those variations of the distribution of charge density in the ionic core that result from different assumptions about the form of the core wave functions in the solid. Thus no unambiguous interpretation of our best estimate of the Fermi energy parameter seems possible; we note, however, that first-principles energy-band calculations lead to values of E_F that are not inconsistent with the present results.

Certain features of the computed values of the partial-wave scattering phase shifts associated with the conduction electron-ion interaction in copper may be understood qualitatively in a simple way. Since there are no f-like core states in copper, the absolute value of the f phase shift is equal to the reduced phase shift. The small positive value (6) corresponds to the fact that the effective one-electron potential in copper is attractive, but much too weak to support an f resonance. The small, negative, d phase shift (6) corresponds to an absolute d phase shift that is somewhat less than π. This result is a consequence of the position of copper at the end of the $3d$ transition series in the periodic table. In potassium, near the beginning of the series, the d phase shift is significantly positive but close to zero,[25] and as an increasing number of d-like states are drawn below the Fermi level, the d phase shift is expected to increase towards π. The absolute values of the s and p phase shifts are determined by adding 3π and 2π, respectively, to the reduced phase shifts. The numerical results (6) bear no simple qualitative interpretation.

A quantitative interpretation of the scattering phase shifts requires some discussion of the form of the effective one-electron potential in copper. We have emphasized that the experimental phase shifts include many-body and relativistic corrections that can be represented only by a nonlocal effective potential, so it is presumably impossible to invert the computed phase shifts in any unique manner to determine the form of the effective potential. However, it is interesting to compare the phase shifts derived from the experimental data with the phase shifts computed from various one-electron potentials that have been proposed for metallic copper. In Table IX(a) the experimental phase shifts are compared with the phase shifts at the same energy derived from the local potential of Chodorow,[32] and from the self-consistent local potential of Snow and Waber.[16] It will be seen that of these two potentials, the Chodorow potential leads to a set of phase shifts in rather better agreement with the phase shifts derived from the experimental data.

If our results for the phase shifts at the Fermi energy are to be taken as the starting point for a calculation of the energy bands in the neighborhood of the Fermi energy in copper, it is convenient to construct a model potential from which the energy dependence of the phase shifts may be derived. It is not difficult to derive a nonlocal model potential that is entirely consistent with the experimental Fermi-surface data. This may be done in a simple way by adding an angular-momentum-dependent potential that is constant within the muffin-tin sphere and zero elsewhere, as a correction to any local potential that is known to give a good first approximation to the experimental Fermi surface. In Table IX(b) we give the nonlocal corrections appropriate to the local potential of Chodorow. Since these corrections are numerically very small, we do not expect the energy bands computed from the modified Chodorow potential to differ greatly from those computed from the local Chodorow potential. We have not carried out a complete band-structure calculation based on the nonlocal potential, but as a simple check we have computed the energy gaps that corre-

spond to those optical transition whose energies have been determined experimentally by Gerhardt.[33] From the results set out in Table IX(c), it can be seen that the energy gaps derived from the modified Chodorow potential agree fairly well with the gaps observed experimentally.[34] There is a small but statistically significant discrepancy between the computed energies corresponding to the higher-frequency transitions, and the experimental data. Presumably this discrepancy could be removed by modifying the local Chodorow potential, which is the starting point for the present calculations, or by allowing an energy-dependent nonlocal correction. Of the various potentials listed in Table IX(c), only the local Chodorow potential rivals our nonlocal potential in predicting optical energy gaps in satisfactory agreement with those observed experimentally. Since the nonlocal Chodorow potential has been constructed to generate a Fermi surface whose dimensions are fully consistent with the experimental data, we believe that it may well prove to be the best available potential for accurate calculations of the band structure of copper close to the Fermi energy.

V. CONCLUSIONS

In this paper, the experimentally observed distortions of the Fermi surface of copper have been analyzed by the phase-shift method. A set of phase shifts for the conduction electron-ion interaction was found, such that the shape of the computed Fermi surface is entirely consistent with the experimental data. The radii computed from the model Fermi surface were found to agree well with the Fermi-surface radii deduced by Halse by an independent technique. This agreement encourages confidence in the results of both calculations, and since the shape of the Fermi surface of copper is strongly influenced by the d-like energy bands that lie just below the Fermi level, it suggests that the phase-shift method may well prove to be of value in analyzing experimental Fermi-surface data for metals of the d-transition series.

From the experimentally observed anisotropy of the de Haas–van Alphen frequency corresponding to the central-belly orbit in copper, it proved possible to estimate the Fermi energy on the APW scale

$$E_F = (0.550 \pm 0.005) \text{ Ry}.$$

This value is consistent with the results of several first-principles band-structure calculations.

The experimental Fermi-surface data were found to imply phase shifts in close agreement with those derived from the local one-electron potential of Chodorow. A small nonlocal correction to the Chodorow potential was proposed, such that the Fermi surface derived from the modified potential is entirely consistent with the experimental data. Certain energy gaps derived from this potential were found to agree to better than 0.2 eV with the gaps measured experimentally by Gerhardt.[33] It seems that the nonlocal potential derived in this way may well prove to be the best available one-electron potential for a full calculation of the electronic energy bands of copper in the vicinity of the Fermi level.

ACKNOWLEDGMENTS

I am grateful to Dr. M. R. Halse and Dr. D. Shoenberg, to K. A. McEwen and Dr. J. Vanderkooy, to E. C. Snow, and to Dr. W. J. O'Sullivan and Dr. J. E. Schirber, for communicating to me their unpublished results. I wish to thank Dr. R. W. Stark for suggesting the graphical technique by which the volume integrals were evaluated, and to thank Dr. U. Gerhardt for a helpful discussion about his optical experiments.

This research was supported in part by the National Aeronautics and Space Administration, and benefited from the use of facilities provided by the Advanced Research Projects Agency for materials research at the University of Chicago. In carrying out this research I was greatly assisted by the use of the facilities of the Computation Center of the University of Chicago.

[33] U. Gerhardt, Phys. Rev. **172**, 651 (1968).

[34] The optical transition energies set out in the last row of Table IX (c) were computed from the modified Chodorow potential, assuming the room-temperature lattice constant quoted by Halse (Ref. 9), namely $a_0 = (3.6147 \pm 0.0003)$ Å.